The silicon-strip tracker of the Gamma ray Large Area Space Telescope

R. Bellazzini*, F. Angelini, R. Bagagli, L. Baldini, A. Brez, M. Ceccanti, J. Cohen Tanugi, M. Kuss, L. Latronico, M.M. Massai, M. Minuti, N. Omodei, G. Spandre, L. Vigiani, F. Zetti

Istituto Nazionale di Fisica Nucleare, University the Pisa, Sezione di Pisa, via Livornese 1291, I-56010 San Piero a Grado (PI), Italy

Abstract

The Gamma ray Large Area Space Telescope (GLAST) is an astro-particle mission that will study the mostly unexplored, high energy (20 MeV–1 TeV) spectrum of photons coming from active sources in the universe. Construction of the GLAST silicon tracker, by far the largest ever built for a space mission, is now well on the way, as it is scheduled for launch by NASA in autumn 2006. We report on the basic technology adopted for the silicon detectors, particularly in connection to their use in space, on the first results of sensors testing and on the status of tracker assembly.
© 2003 Elsevier B.V. All rights reserved.

Keywords: High-energy astrophysics; Silicon-strip tracker; Gamma ray

1. Introduction

Gamma rays are one of the deeper probes into nature's highest-energy processes. Due to their small interaction cross-section, they potentially offer a direct view into the most distant energetic sources; moreover, unlike cosmic rays, they are not affected from intergalactic magnetic fields. Unfortunately technological difficulties have prevented for a long time the effective exploitation of astronomy within this energy band. After some pioneering missions (OSO III, SAS-2, COS-B), the

Energetic Gamma Ray Experiment Telescope (EGRET), launched in 1991, has performed the first complete survey of the gamma ray sky above 30 MeV, finding it surprisingly dynamic and various. The most recent EGRET catalog includes 271 point sources. Among them 170 remain unidentified (no counterparts are known at other wavelengths). The others are incredibly diverse, ranging from Active Galactic Nuclei to Pulsars and Supernova Remnants.

GLAST capabilities will greatly exceed those of previously flown instruments, providing an unprecedented advance in sensitivity. GLAST will presumably discover thousands of AGN and hundreds of gamma ray pulsars. Precise time-resolved spectral measurements will likely allow to

*Corresponding author.

E-mail address: ronaldo.bellazzini@pi.infn.it (R. Bellazzini).

throw light on particles acceleration and gamma ray production mechanisms in these source classes. Short dead time will permit detailed study of transient sources, opening exciting prospectives for Gamma Ray Burst (GRB) physics. In addition to this, a great localization power will allow a precise removal of the contribution of point sources to the extragalactic gamma background detected by EGRET; a truly diffuse remaining component would have a great cosmological interest and would rank as one of the most important discoveries of GLAST.

2. The Gamma ray Large Area Space Telescope

The GLAST mission is basically intended to allow a systematic study of the gamma ray sky in the energy band that ranges from 20 MeV up to the TeV scale. It will raise up the EGRET high energy sensitivity limit ($\simeq 10$ GeV) and it will provide the overlap to the ground based telescopes [1]. Such a various physical scenario imposes strict instrumental requirements: a short dead time for transient studies, a good energy resolution over a broad energy band and a large field of view with excellent angular resolution to achieve high sensitivity with great localization power. In addition to this, the space environment requires the use of robust and proven technology (possibly free from consumables), modular and redundant overall design and low power consumption. There is no doubt that the achievement of so many different requirements constitutes a great scientific and technological effort for the astrophysics and particle physics communities involved in the project.

2.1. The Large Area Telescope

The Large Area Telescope (LAT), the main instrument onboard GLAST, is a gamma ray telescope based on the pair production effect, which is the photon interaction process with the greatest cross-section in GLAST energy range. The direction of incoming photons will be derived by reconstructing the two electron tracks in a high resolution silicon-strip tracker. The photon energy will be measured in a CsI imaging electromagnetic calorimeter (10 radiation lengths), while the rejection of charged particles background (outnumbering gamma ray flux by more than five orders of magnitude) will be granted by an outer, segmented Anti Coincidence Detector (ACD). The LAT has a fully modular architecture; it consists of a 4×4 array of identical towers each one comprising a tracker, a calorimeter and a Data Acquisition Module, with a total power consumption of 580 W.

2.2. The GLAST silicon tracker

As the whole instrument, the GLAST silicon-strip tracker (Fig. 1) is modular in its structure, consisting of 16 tower modules each one with 37 cm $\times$ 37 cm active cross-area [2,3]. In order to minimize the number of readout channels, sensors are glued edge to edge and wire bonded together in groups of four to form a unique detector (89.5 mm $\times$ 358 mm); these substructures are called *ladders*. Ladders are then glued onto trays structures which constitute the basic mechanical frame and contain tungsten converter foils; detection planes (two per tray, with the same orientation) are made up by 4 ladders.
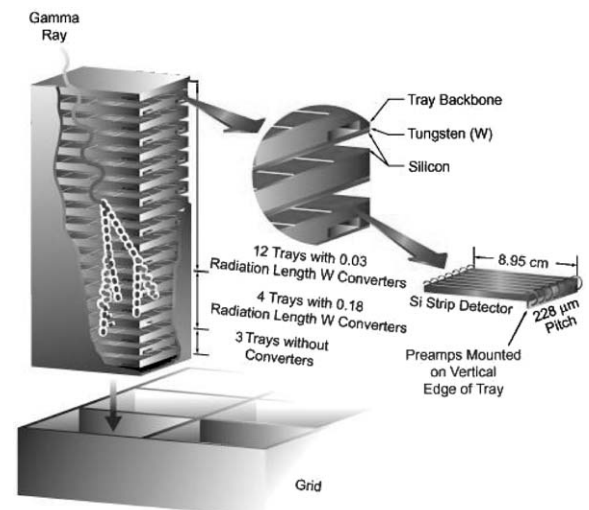

Fig. 1. Modular structure of the Large Area Telescope silicon tracker.

There are 19 trays structures per tower: 12 with 3% radiation length conversion foils, 4 with 18% radiation length and 3 (the closest to the calorimeter) with no converter at all. Every other tray is rotated by 90° with respect to the previous one in such a way that each W foil is immediately followed by a x–y plane of detectors for vertex reconstruction. Electronics lies on sides of the trays, in order to minimize the gap between the towers; there are 9 readout modules on each of the four sides. The full GLAST tracker will contain about 10 500 silicon sensors, over 83 m^2 of covered area, for a total of more than 1 million electronic channels.

2.3. The GLAST silicon sensors

The GLAST sensors [5,4] must be simple, cost effective and reliable; they have to provide high detection efficiency and large S/N ratio allowing high resolution tracking with a low defect density. Silicon strip technology, which has a long and successful history of application in accelerator based high energy physics, has been chosen for this extremely large scale space application.

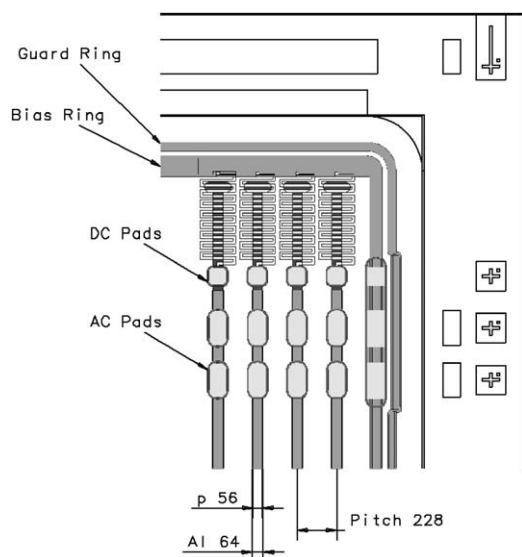A schematic layout of one corner of the GLAST silicon-strip detectors is shown in Fig. 2. The use

Fig. 2. Schematic layout of one corner of GLAST Silicon Strip Detectors. Quoted dimensions are intended in μm.

of the 6″ technology has allowed to reduce the number of SSDs to be procured by one half, if compared with the usual 4″ technology, allowing considerable cost and time savings in the tray assembly. This choice has also limited the list of potential manufacturers to few companies with whom an intense prototyping activity has started. Criteria of the prototyping program have been simplicity and robustness of design, high quality, predictability and uniformity of performance, ease of testing. Sensors have been obtained from high resistivity (> 5 kΩ/cm) wafers; they are single sided, AC coupled and passivated with glass. 384 p$^+$ strips (56 μm wide) are implanted on a 400 μm thick n-type substrate and biased through polysilicon resistors. The total active area is 87.5 mm × 87.5 mm. The 400 μm substrate thickness results from the optimization of different and somewhat conflicting requirements, such as good S/N and vertexing, low multiple scattering and bias voltage. For each strip there are two AC pads for wire bonding (on the Al decoupling electrode) and one DC pad (contacting the implant) for testing purposes. A 228 μm strip pitch has been chosen as the ideal compromise between tracking resolution, reduction of necessary electronics readout channels, power consumption and reliability. The increase of the pitch with respect to the initial value of 201 μm results in a tracker power saving of 12% but also in a worsening of the high-energy Point Spread Function for normal incidence and of the high latitude point source sensitivity of approximately 5% and 3%, respectively. The effect of the pitch change on the PSF, for a 68% containment space angle, is more pronounced at higher energies where the multiple scattering is somewhat less important and it is shown in Table 1. The moderate wider pitch has also a somewhat small but negative effect on instrument performances like the two-track separation capability and hence the background rejection. Theoretically, the hit efficiency at large track angle should improve with a wider pitch and this fact should help the background rejection, increase the effective area and reduce PSF tails. We also note that the spatial positioning error introduced by multiple scattering in tungsten conversion foils would unlikely allow to fully exploit advantages of

Table 1
The power consumption and savings for different pitches in the TKR. Increasing the pitch by 40% increases the PSF(68) by 12% at 10 GeV and decreases the power by 24%

Pitch (μm)	PSF (68) (deg)			TKR Power (W) (Change (%))	Signal increase @80 deg incidence
	0.1 GeV	1.0 GeV	10 GeV		
201	3.17	0.40	0.081	210 (0)	0
235	3.24	0.41	0.085	184 (−12)	17
282	3.26	0.42	0.091	159 (−24)	40

Table 2
Defect analysis provided by manufacturer; a total of 105 bad strips out of 1101312 (less than 10^{-5}) has been found

Defect type	Number
Coupling short	45
Strip isolation	2
DC	19
Al short	6
Al open	3
Implant open	7
Implant short	2
Leaky strip	5
Polysilicon resistors	12
Strip open	3
Total	105

a smaller strip pitch. The implant width has also been adjusted to keep the electric field on the implants in a safe region.

3. Wafers testing

Sensors production has started full stream. 2868 detectors, representing about 25% of the total, have been already received from Hamamatsu Photonics. To date, this is the largest gathered silicon-strip detector surface (about 23 m^2). Wafers are preliminarily tested from the manufacturer for:

- number of defective channels and type of defects (Table 2),
- average values of bias polysilicon resistors, strip decoupling capacitance and Al resistance from one sample detector per batch and
- total leakage current and bulk capacitance as a function of bias voltage.

Single strip tests, which are extremely time-consuming are not repeated at the level of wafer acceptance-testing thanks to the impressive uniformity of SSDs characteristics within each batch and the high quality of the production. Total current measurements and bulk capacitance scans are instead repeated in order to verify that no damages have been occurred in packing and shipping operations.

In the next section the detectors acceptance testing procedures performed in the Italian collaboration labs are described. At receiving, sensors are stored in controlled N_2 atmosphere cupboards and all measurements are done in a class 10 000 clean room.

3.1. Electrical tests

By comparing the individual strip leakage currents with the total current on the same SSD, a close correlation between anomalous high total leakage current and excessive high current on a single strip has been found. In this way the number of noisy strips can be monitored simply through the fast measurement of the total leakage current. As electrical quality check the total leakage current (I–V curve) and the bulk capacitance (C–V curve) are measured for each detector at different bias voltages with a light-tight probe station. In both measurements all strips are grounded while the backplane is connected to a variable positive voltage (0–200 V). The sensor specifications for acceptance [6] require, to reduce the shot noise due to 35 cm strip length, an average leakage current less than 200 nA at 150 V with a maximum value of 500 nA. Furthermore, for power consumption and noise reduction, a low full depletion voltage (<120 V) is required. The operation of sensors under low bias voltages is desirable for a space mission where limited power and potential for arcing are a problem. According to the specifications the breakdown voltage, marked by a change of slope in I–V curve, should be > 175 V. A total
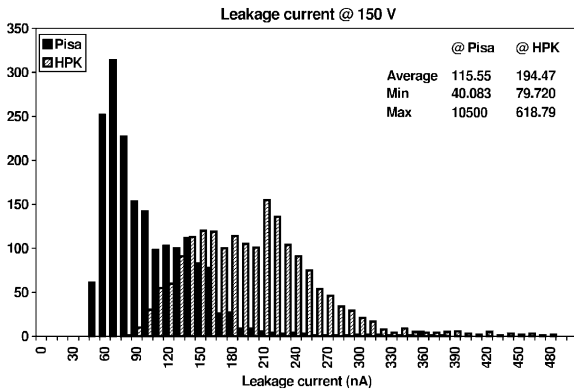
Fig. 3. Measured leakage current at 150 V (at HPK and in Pisa) for all tested detectors. Differences are due to temperature/humidity effects and to the fact that manufacturer measures current before cut, just after processing. An increase in temperature of 7.5°C causes an increase of the leakage current by a factor two [7].
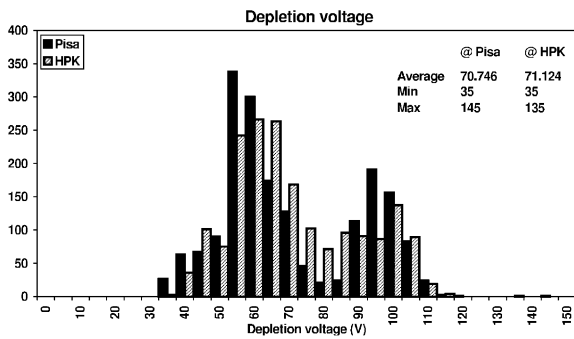

Fig. 4. Measured depletion voltage (at HPK and in Pisa) for all tested detectors.
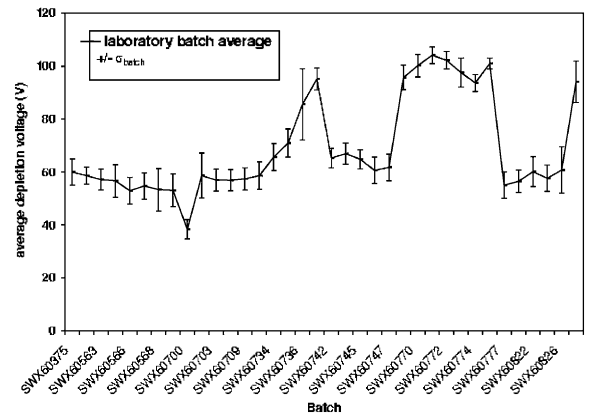

Fig. 5. Average values and standard deviations of measured depletion voltages within different production batches.

Table 3
Summary of rejected wafers

Non conformance type	Number of rejected sensors
High leakage current	13
Low breakdown voltage	5
High depletion voltage	1
Chipped corner	3
Mishandling	2
Total	24

of 1811 detectors (more than 15% of the total production) have been completely electrically tested. Fig. 3 shows the resulting distribution of the leakage currents. Only 18 sensors were found out of specification for bad $I–V$ curve, while the average current is slightly above 1 nA/cm^2 at 25°C indicating a very mature fabrication process.

The value of full depletion voltage is deduced from $C–V$ curve; it is defined as the voltage step for which

$$\frac{1}{C^2(V)} - \frac{1}{C^2(V-5)} < 0.0039 nF^{-2}. \qquad (1)$$

In Fig. 4 the distribution of measured depletion voltages is reported; only one sensor was found out of specifications for bad $C–V$ curve. The average depletion voltage is about 70 V that satisfies the required specifications. This depletion voltage is relatively low for a 400 μm substrate thickness and it is due to the use of high resistivity wafer. The difficulty in controlling the resistivity at high values is the reason why the full depletion voltage spreads so much. Nevertheless it is worth noticing the impressive uniformity of the depletion voltage values within each production batch (Fig. 5), which largely simplifies the wafer selection procedure for ladders assembly.

Table 3 summarizes the results of the performed tests. 24 sensors in total (about 1.3%), out of 1811 tested, have been definitively rejected; the table also includes some wafers with chipped corners (probably due to problems during transport) and others damaged during tests.
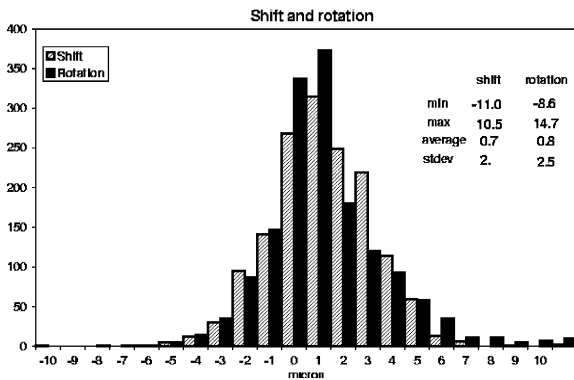
Fig. 6. Distributions of the two parameters (shift and rotation) measured in geometrical tests.

Fig. 7. Wafers alignment errors within 140 mechanical ladders assembled for the Engineering Model Tower.

3.2. Geometrical tests

Each sensor undergoes geometrical test to check the precision of wafer cut, which represents the mechanical reference during ladder assembly. According to the contract requirements, the maximum allowed cut error is 20 μm. The distances between the center of reference crosses (situated on each corner) and the edges of detector are measured using a computerized CCD camera mounted on a microscope. The whole system is calibrated on the length of the cross itself, assuming sub-micron precision of the lithography. The wafer is moved by a computer controlled XY table. Since the field of the picture (about 500 μm × 300 μm) is wide enough to contain the reference cross and the edges, the error on the measurement is only determined by the pixel size, which is less than 1 μm. The alignment of the strips to the edge (rotation) and their mean distance from the nominal position (shift) are evaluated. Fig. 6 summarizes the results. Not a single detector (out of 1531 tested) was found out of geometrical specifications.

4. Tracker construction status

4.1. Ladder assembly

Ladders construction basically involves the following steps:
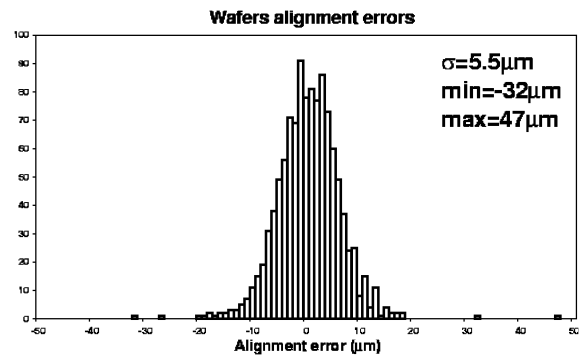
- head to head gluing of four wafers,
- mechanical survey of relative alignment,
- wire bond of sensors and encapsulation of wire bonds and
- electrical tests on ladders.

The good uniformity of the silicon sensors resulting from the qualification tests allows a fast selection for ladder assembly. Sensors belonging to the same production batch have very similar depletion voltages and leakage currents, so ladders can be easily built using detectors from the same batch or from batches with similar properties. The alignment of wafers within a ladder has to be better than 40 μm. A total of 140 ladders from mechanical wafers have been produced for the Engineering Model Tower. The resulting alignment errors are shown in Fig. 7. After assembly, sensors are wire bonded; space applications require wire bonds to be encapsulated. Finally assembled ladders have to undergo electrical test to check their integrity. Flight ladders production is now starting. Electrical behavior during all stages of assembling procedure has been monitored for some prototypes. As shown in Fig. 8, no substantial increase of leakage current (with respect to the sum of single wafer current) has been observed.

4.2. Trays and towers construction

A great effort has been taken in trays design. Basic structure and choice of materials are now well established. High technology materials, such
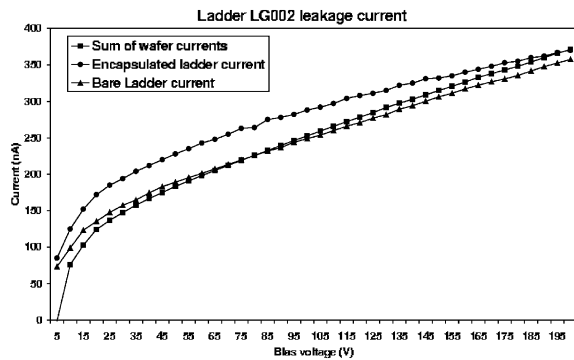
Fig. 8. Leakage current measured in different stages of ladder assembly.

as carbon fiber and carbon–carbon, are used. They ensure torque and mechanical stress resistance, high thermal conductivity for heat dissipation and low material budget. Some prototype trays have already been assembled. The tray planarity has been measured to be less than 20 μm and the machining precision on the overall outer dimensions $\simeq 50$ μm (over $\simeq 37$ cm), well within the required tolerances. A set of thermal and vibrational tests, crucial for space applications, has begun as well.

Upon completion of the tower assembly and prior to launch, the full LAT tracker will be calibrated with cosmic rays, both at ground level and on airplane, as well as with charged particles and photons beams. Periodic dedicated runs to assess the status of dead and noisy channels, single hit efficiency and Time Over Threshold calibration are foreseen during satellite operation.

5. Conclusions

From the science point of view, GLAST will provide a flood of high quality data with which to study the high energy gamma ray sources in the Universe. From the point of view of technology, GLAST will be one of the largest applications of the silicon-microstrip detector technique, in a different environment from the HEP accelerators for which it was initially developed. Construction of the GLAST silicon-strip tracker is now well on the way. Wafer procurement is properly scheduled and has already reached about 25% of the total production. Tests on sensors proceed at full rate, pointing out the excellent uniformity, well within specifications, of the production activity; flight ladders assembly has started as well, with very good preliminary results. Basic technological choices and working procedures for what regards trays and tower assembly are, to date, definitively established and tests on prototypes have already begun.

References

[1] E. Bloom, G. Godfrey, S. Ritz, Proposal for the Gamma-ray Large Area Space Telescope, SLAC-R-22, February 1998.
[2] E. Atwood, et al., Nucl. Instr. and Meth. A 457 (2001) 126.
[3] W.B. Atwood, et al., Nucl. Instr. and Meth. A 435 (1999) 224.
[4] R. Johnson, GLAST LAT Technical Document, LAT-TD-00156-1.
[5] F. Hartmut, et al., GLAST LAT Technical Note, LAT-TD-00070-01.
[6] H. Sadrozinski, T. Ohsugi, GLAST LAT Procurement Specification, LAT-DS-00011-10.
[7] T. Ohsugi, et al., Nucl. Instr. and Meth. A 436 (1999) 272.